Molecular and Ultrastructural Defects in a *Drosophila* Myosin Heavy Chain Mutant: Differential Effects on Muscle Function Produced by Similar Thick Filament Abnormalities

Patrick T. O'Donnell and Sanford I. Bernstein

Biology Department and Molecular Biology Institute, San Diego State University, San Diego, California 92182

Abstract. We have determined the molecular defect of the *Drosophila melanogaster* myosin heavy chain (MHC) mutation *Mhc*^{1} and the mutation's effect on indirect flight muscle, jump muscle, and larval intersegmental muscle. We show that the *Mhc*^{1} mutation is essentially a null allele which results in the dominant-flightless and recessive-lethal phenotypes associated with this mutant (Mogami, K., P. T. O'Donnell, S. I. Bernstein, T. R. F. Wright, C. P. Emerson, Jr. 1986. *Proc. Natl. Acad. Sci. USA.* 83:1393–1397). The mutation is a 101-bp deletion in the MHC gene which removes most of exon 5 and the intron that precedes it. S1 nuclease mapping indicates that mutant transcripts follow two alternative processing pathways. Both pathways result in the production of mature transcripts with altered reading frames, apparently yielding unstable, truncated MHC proteins. Interestingly, the preferred splicing pathway uses the more distal of two available splice donor sites. We present the first ultrastructural characterization of a completely MHC-null muscle and show that it lacks any discernable thick filaments. Sarcomeres in these muscles are completely disorganized suggesting that thick filaments play a critical role in sarcomere assembly. To understand why the *Mhc*^{1} mutation severely disrupts indirect flight muscle and jump muscle function in heterozygotes, but does not seriously affect the function of other muscle types, we examined the muscle ultrastructure of *Mhc*^{1}/+ heterozygotes. We find that these organisms have a nearly 50% reduction in the number of thick filaments in indirect flight muscle, jump muscle, and larval intersegmental muscle. In addition, aberrantly shaped thick filaments are common in the jump muscle and larval intersegmental muscle. We suggest that the differential sensitivity of muscle function to the *Mhc*^{1} mutation is a consequence of the unique myofilament arrays in each of these muscles. The highly variable myofilament array of larval intersegmental muscle makes its function relatively insensitive to changes in thick filament number and morphology. Conversely, the rigid double hexagonal lattice of the indirect flight muscle, and the organized lattice of the jump muscle cannot be perturbed without interfering with the specialized and evolutionarily more complex functions they perform.

ANALYSIS of muscle mutants offers a powerful approach to understanding muscle assembly, development, and function. This is particularly the case for the fruit fly *Drosophila melanogaster* and the nematode *Caenorhabditis elegans*, where ultrastructural, physiological, and molecular analyses can be aided by the relative ease of mutant isolation and manipulation. In both of these organisms, mutations that affect muscle structure and function, but not viability, can be readily isolated. In *Drosophila*, the function of the indirect flight muscle (IFM)[1] and the jump or tergal depressor of the trochanter muscle (TDT) are not essential to viability or fertility. Likewise, the body wall muscle of *C. elegans* is not essential, since nonmotile organisms can feed and digest. In *C. elegans*, mutations of structural genes encoding myosin heavy chain (MHC) (MacLeod et al., 1977*a*,*b*; Dibb et al., 1985), paramyosin (Waterston et al., 1977), and actin (Waterston et al., 1984; Landel et al., 1984), as well as apparent regulators of these genes (Mackenzie et al., 1978) have been described.

Previously, we and others have shown that tl *Drosophila* muscle MHC gene is single copy in the haploid genome and is regulated in a stage and tissue-specific manner (Bernstein et al., 1983, 1986; Rozek and Davidson, 1983, 1986). Haploidy of the MHC region at polytene chromosome locus 36AC(2L) results in the reduction of MHC protein in all muscle types (Bernstein et al., 1983). Although most muscles function in these haploids, flight and jump muscle functions are severely disrupted. The sensitivity of flight and jump muscle function to gene dosage extends to other contractile protein genes as well. This has permitted the isolation of dominant mutations which result in a flightless phenotype

1. *Abbreviations used in this paper*: IFM, indirect flight muscle; MHC, myosin heavy chain; TDT, tergal depressor of the trochanter muscle.

(Mogami and Hotta, 1981). Characterization of these dominant muscle mutations indicates they fall into two categories: homozygous-viable mutations that affect protein isoforms specific to the IFM (Karlik et al., 1984; Karlik and Fyrberg, 1985; our unpublished results), and mutations that when homozygous lead to embryonic or early larval lethality (Mogami et al., 1986).

Drosophila, in addition to being amenable to genetic and molecular analyses of muscle development, provides excellent systems of muscle fibers in which to investigate the consequences of mutations within myofibrillar genes (see Crossley, 1978; Miller, 1950 for a summary of *Drosophila* muscle anatomy). In adult flies most of the thorax is occupied by the IFM, a series of 26 muscle fibers which function to produce primary movements of the wings by changing the shape of the thorax. The IFM of insects has evolved specialized features which allow it to produce wing beat frequencies of 300 Hz or greater. IFM fibers contain highly ordered myofibrils (Cullen, 1974; Garamvolgyi, 1965*a*,*b*; Peristianis and Gregory, 1970; Shafiq, 1963*a*,*b*) and large mitochondria which occupy 30–40% of fiber volume (Shafiq, 1963*a*,*b*; Smith, 1963). These muscles display asynchronous contraction; a single burst from motor neurons causes initial activation and this active state is maintained by rapid changes in length and tension that result from the mechanical properties of the muscle itself (Nachtigall and Wilson, 1967; Pringle, 1967; Thorson and White, 1969; Tregear, 1975). Another major thoracic muscle is the TDT that inserts on the mesothoracic legs and the dorsal cuticle. The power required for jumping is achieved by the storage of energy resulting from the slow contraction of the TDT, followed by its sudden release (Chapman, 1982). At the larval stage, the major muscle type consists of 28 segmentally repeated pairs of hypodermal muscles (Crossley, 1978). These muscles are attached at each intersegmental line and work coordinately to produce larval movement (see Toselli and Pepe, 1968*a*, *b*; Crossley, 1968 concerning structure of insect hypodermal muscle). Comparing the structure of mutant and wild-type *Drosophila* muscles can provide important insights in defining the genetic lesion caused by a particular mutation (Mogami et al., 1981).

The *Mhc*^{1} mutant was isolated in a screen for dominant mutations which affect IFM function. Chromosomal mapping indicated that the *Mhc*^{1} mutation, along with a number of additional dominant flightless mutations, map to the 36AC chromosomal region near the MHC gene (Mogami and Hotta, 1981; Mogami et al., 1986). *Mhc*^{1} homozygotes are capable of undergoing gastrulation but die at the late embryonic stage without displaying muscular movement (Mogami et al., 1986). *Mhc*^{1} heterozygotes accumulate 60% of the normal amount of MHC protein in leg muscle and IFM. Southern blot analysis indicates there is a small deletion near the 5′ end of the MHC gene of this mutant (Mogami et al., 1986).

In this paper we examine the molecular nature of the *Mhc*^{1} mutation and determine its effect on the myofibrillar structure of the IFM, TDT, and larval intersegmental muscle. We were particularly interested in examining why this mutation, which affects MHC accumulation in all muscle types, severely disrupts only IFM and TDT function in heterozygotes. We show that *Mhc*^{1} is essentially a null allele which results from an altered translational reading frame. This apparently leads to the production of unstable, truncated MHC proteins. Examination of IFM, TDT, and larval intersegmental muscle of *Mhc*^{1}/+ heterozygotes indicates the *Mhc*^{1} mutation reduces the number of thick filaments by nearly 50% in each of these muscle types. IFM and TDT muscle functions are apparently more sensitive to the *Mhc*^{1} mutation as a consequence of their highly ordered myofilament and myofibrillar arrays which have evolved to perform more complex functions.

The existence of only a single muscle MHC gene which encodes all isoforms of the protein in conjunction with the null nature of the *Mhc*^{1} mutation has afforded us the unique opportunity to observe the ultrastructural phenotype of completely null MHC muscle. We show that in the absence of MHC, no distinguishable thick filaments are present and sarcomere construction is severely retarded.

Materials and Methods

Materials

Restriction enzymes, RNase A, proteinase K, DNA ligase, DNA polymerase, T4 polynucleotide kinase, calf intestinal phosphatase, DNase I, and S1 nuclease were from Bethesda Research Laboratories (Gaithersburg, MD), Boehringer Mannheim Diagnostics, Inc. (Houston, TX), or New England Biolabs (Beverly, MA). Lambda gt10, lambda packaging extracts, and *Escherichia coli* strain *C600hfl*$^-$ were from Stratagene (La Jolla, CA). Paraformaldehyde, glutaraldehyde, Spurr's embedding medium, uranyl acetate, and lead citrate were from Ted Pella, Inc. (Irvine, CA). Autoradiography enhancer and [^{35}S]methionine were from New England Nuclear (Boston, MA). Nucleoside triphosphates were from Amersham Corp. (Arlington Heights, IL). NA45 paper was from Schleicher and Schuell, Inc. (Keene, NH). Most reagent grade molecular biology reagents were from Bethesda Research Laboratories.

Isolation of Drosophila DNA

Mhc^1/+ DNA was prepared from adult *Drosophila*. One gram of flies was homogenized in 15 ml of homogenization buffer (100 mM NaCl, 30 mM Tris-HCl, pH 8.0, 10 mM EDTA, 10 mM β-mercaptoethanol, 0.5% Triton X-100) in a 15 ml glass-on-glass homogenizer (Wheaton Scientific Industries, Millville, NJ). Adult flies were first homogenized using a pestle with a larger clearance and then a pestle with a smaller clearance. Nuclei were pelleted by centrifuging the homogenate at 1,500 *g* for 20 min at 4°C. Nuclei were resuspended in 5 ml of resuspension buffer (100 mM Tris-HCl, pH 8.4, 20 mM EDTA, 100 mM NaCl). 500 μl of 10% SDS and 2 mg of proteinase K were added, and the sample was incubated overnight at 37°C. The sample was then phenol-chloroform extracted until the interface was clear. DNA was precipitated by adding 0.04 vol of 5 M NaCl and 2 vol of ethanol. After storage at −70°C for 30 min, the DNA was pelleted by centrifugation at 1,000 *g* for 5 min. To remove RNA, the pellet was resuspended in 4 ml of 0.1× SSC (15 mM NaCl, 1.5 mM Na Citrate) and 20 μl of 20 mg/ml preboiled RNase A was added. After incubation at 37°C for 45 min the sample was phenol-chloroform extracted and dialyzed overnight against 4 liters of TE (10 mM Tris-HCl, pH 8.0, 1 mM EDTA). DNA was ethanol precipitated as before, dried in vacuo, and finally resuspended in TE.

Cloning of the Mhc^1 Gene

40 μg of *Mhc*^{1}/+ DNA was completely digested with Eco RI and size fractionated on a 0.8% agarose gel. Eco RI fragments from 4–6 kb were then electrophoresed onto NA-45 paper that had been briefly wetted in TE. DNA was eluted from NA-45 paper by incubating in 500 μl of elution buffer (1 M NaCl, 50 mM Tris-HCl, pH 8.0, 1 mM EDTA) at 70°C for 5 h. The sample was phenol-chloroform extracted and the DNA precipitated by adding 0.6 vol of isopropanol. 0.2 μg of this DNA was ligated to 2 μg of Eco RI-digested lambda gt10 vector in a 10-μl ligation reaction overnight at 4°C (Maniatis et al., 1982). After packaging of ligation products, phage harboring inserts were selected by plating on *E. coli* strain *C600 hfl*$^-$. After plating, plaques were screened by transferring to nitrocellulose and hybridizing (Maniatis et al., 1982) to a nick-translated portion of the wild-type MHC

gene. Positive plaques were further characterized by restriction digest of "mini" DNA preparations of bacteriophage DNA (Maniatis et al., 1982). *Mhc*^{1} clones were differentiated from wild-type clones based on the presence of a smaller Bam HI fragment (Mogami et al., 1986).

DNA Sequencing and S1 Nuclease Mapping

DNA sequencing was performed by the method of Maxam and Gilbert (Maxam and Gilbert, 1980) as previously modified (Bernstein et al., 1986). S1 nuclease mapping was performed as described by Wassenberg et al. (1987). DNA sequences and S1 nuclease-protected fragments were electrophoresed on urea–polyacrylamide gels (Maxam and Gilbert, 1980).

MHC Protein Analysis

To examine MHC protein accumulation in *Mhc*^{1}/+ and *Canton Special* (wild-type) organisms, three female thoraces were homogenized in 70 μl of SDS sample loading buffer (Laemmli, 1970). After boiling, 35 μl of the final volume was loaded onto a 12.5% polyacrylamide gel containing SDS (Laemmli, 1970). After electrophoresis, the gels were stained with Coomassie Brilliant Blue. To analyze MHC protein synthesis in *Mhc*^{1}/+ and *Canton-S*, three female pupae were each injected with 0.5 μl of [^{35}S]methionine (1,000 Ci/mmol) using a pulled microcapillary pipette. The pupae were then incubated for 1 h in a moist glass petri dish. Thoraces were then dissected, homogenized in SDS sample buffer, and electrophoresed as described above. After electrophoresis, gels were treated with an autoradiography enhancer agent (Enhance), dried, and exposed to film. *Mhc*^{1}/+ lanes were compared with *Canton-S* (wild-type) lanes for the presence of additional band(s).

Electron Microscopy of Muscles

Homozygous *Mhc*^{1} embryos were prepared for fixation as follows. *Mhc*^{1}/*Cy* flies were mated and allowed to lay eggs for 5 h on 1.2% agar plates containing 25% grape juice and a smear of yeast. The embryos were then collected from the plates and dechorionated by treating with 1.25% sodium hypochlorite (bleach) for 4 min. After dechorionation, the embryos were rinsed with water and allowed to incubate for 24 h at room temperature in a petri dish containing water. Embryos were then examined under a dissecting microscope and homozygous *Mhc*^{1} larvae were identified by their failure to move within the egg membrane. The membrane was removed from these embryos by rolling each egg with a pair of forceps. *Canton-S* embryos were collected in the same manner, except that larvae were able to hatch during the 24-h incubation period. These were collected and immediately placed in the initial fixative. First instar larvae were fixed in 1.5-ml microcentrifuge tubes as described below. Final embedding was done in 0.5-ml microcentrifuge tubes.

Fixatives do not efficiently permeate the cuticle of either larvae or adults and therefore it is necessary to pierce the cuticle or dissect the muscles of interest with a double-edge razor blade before fixation. For first instar larval preparations, the cuticle was pierced with forceps. Third instar larvae were first exposed to ether vapor to ensure muscle relaxation. They then were pinned to a paraffin wax block in a slightly stretched state. After pinning, larvae were bisected anterior to posterior and exposed to fixative for 15 min. Pins were then removed and the larvae were transferred to fresh fixative overnight as described below. For IFM and TDT preparations, the head and abdomen were first removed and then thoracic regions not containing the muscle of interest were dissected away. The remaining tissue was placed in fixative as described below.

A fixative containing paraformaldehyde and glutaraldehyde was used for the initial fixation of all muscle types (3% paraformaldehyde, 2% glutaraldehyde, 100 mM sucrose, 100 mM sodium phosphate buffer, pH 7.2, 2 mM EGTA). Samples were treated with the initial fixative overnight at 4°C. Samples were then washed for 45 min in 100 mM sodium phosphate buffer, pH 7.2, and treated with a postfixative (1.0% osmium, 100 mM sodium phosphate, pH 7.2) for 2 h at 4°C. After osmium treatment, samples were washed in distilled water for 45 min at 4°C and then dehydrated in acetone at room temperature. Samples were embedded in Spurr's resin (Spurr, 1969). To improve resin permeation, samples were placed in 75% Spurr's, 25% acetone, and held under vacuum for 3 h. Samples were then transferred to 100% Spurr's for 1 h before final embedding. Sections were cut with a glass or diamond knife (EM Science Corp., Chestnut Hill, MA). Sections were stained for 20 min in 2% aqueous uranyl acetate, pH 4.5, followed by lead citrate for 4 min.

Results

Molecular Nature of the Mhc^1 MHC Mutation

We previously initiated the investigation of the molecular nature of the *Mhc*^{1} mutation (Mogami et al., 1986). DNA from the mutant was digested with a number of restriction enzymes and Southern blots were performed using the nick-translated MHC gene. Comparison of the genomic DNA restriction fragments from *Mhc*^{1}/+ heterozygotes with those of the parental (*Canton-S*) strain revealed evidence of a small deletion in the MHC gene of the mutant *Mhc*^{1}. The deletion gives rise to Bam HI and Sal I restriction fragments that are detectably shorter than wild-type fragments. The arrangement of the Bam HI and Sal I restriction sites within the wild-type MHC gene is such that the deletion must map to a region between the two restriction sites, a distance of ~400 bp. To precisely define the molecular defect of the *Mhc*^{1} allele, we cloned the mutated region by preparing a lambda phage gt10 library from genomic DNA of *Mhc*^{1}/+ heterozygotes. From a screen of 1×10^5 recombinants (5% of the library), we recovered 15 positive clones. We made mini preparations of bacteriophage DNA from six of these. Bam HI digests of DNA from the six lambda clones indicated that three possess the shorter restriction fragment indicative of the *Mhc*^{1} mutation. We subcloned the entire insert consisting of a 5.5-kb Eco RI fragment from one of these clones into the plasmid *pUC* 19 for sequencing.

DNA sequencing showed that the *Mhc*^{1} mutation is a 101-bp deletion within the MHC gene (Fig. 1). We previously determined the nucleotide sequence for the 5′ end of the wild-type *Drosophila* muscle MHC gene (Wassenberg et al., 1987). Using S1 nuclease mapping, primer extension experiments, knowledge of consensus splice junctions, and the encoded amino acid sequences of other MHC genes, we had derived the location of the first five exons of the *Drosophila* MHC gene. The region that is deleted by the *Mhc*^{1} mutation encodes the ATP binding site for the MHC protein. As can be seen in Fig. 1, the deletion removes most of exon 5 and the preceding intron.

Since the *Mhc*^{1} mutation removes the splice acceptor site from exon 5, we were uncertain regarding the RNA processing pathway used by the mutant transcripts. The deletion creates a situation where the donor sites of exon 4 and 5 are competing for the acceptor site of exon 6. We performed an S1 nuclease protection experiment to determine which of the two donor sites is used in the splicing of *Mhc*^{1} mutant transcripts. A DNA fragment was 3′ end–labeled at its upstream Sal I site, hybridized to *Mhc*^{1}/+ pupal RNA, and then treated with S1 nuclease. The protected fragments were separated by gel electrophoresis in parallel with a DNA sequence beginning at the labeled Sal I site. Transcripts using the donor site of exon 4 would yield a protected fragment of 239 bases, while transcripts using the donor site of exon 5 would yield a protected fragment of 275 bases. Our results (Fig. 2) indicate that nearly all of the transcripts in *Mhc*^{1}/+ flies use the donor site of exon 4. A very small percentage of the transcripts possess the longer protected fragment resulting from the use of the donor site of exon 5. Results of this analysis are complicated by the presence of wild-type MHC RNA in *Mhc*^{1}/+ heterozygotes. Wild-type transcripts always use the donor site of exon 4. It was therefore possible that mutant

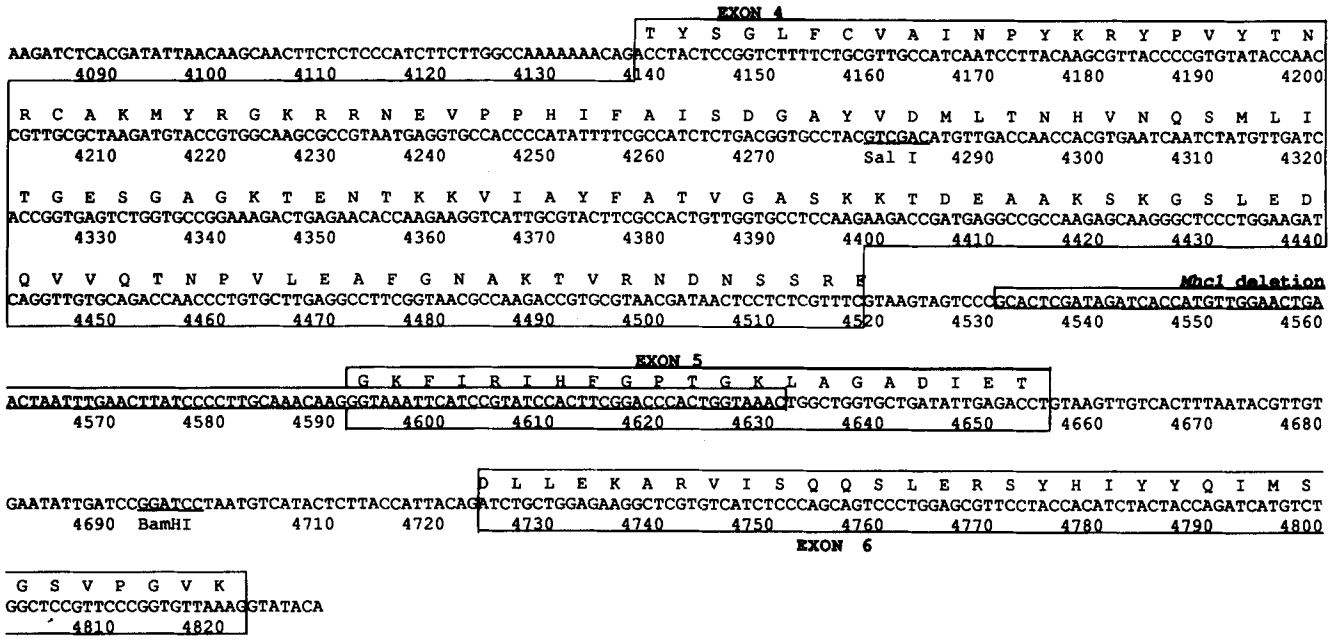

Figure 1. Sequencing of the *Mhc*^{1} mutation indicates it is a 101-bp deletion which removes most of exon 5 (40/64 nucleotides) and the intron preceding it. Position of the *Mhc*^{1} mutation and the DNA sequence and derived amino acid sequence of the wild-type *Drosophila* MHC gene for exons 4, 5, and 6 are shown. The nucleic acid numbering system follows that of Wassenberg et al. (1987). Exons and the sequence deleted in the *Mhc*^{1} mutation are boxed and labeled. The *Mhc*^{1} mutation had previously been shown to lie between Bam HI and Sal I restriction sites (Mogami et al., 1986), which are indicated. The Sal I restriction site was 3′ end-labeled for the S1 nuclease protection experiment shown in Fig. 2.

transcripts exclusively used the donor site of exon 5, but that these transcripts were unstable relative to wild-type mRNAs. To examine this possibility, we performed an S1 protection experiment using RNA isolated from homozygous *Mhc*^{1} embryos. We again found that the vast majority of mutant transcripts use the donor site of exon 4 (data not shown).

Most *Mhc*^{1} transcripts use the donor splice site of exon 4 which results in the omission of exon 5 sequences. This leads to a change in the translational reading frame that is +1 relative to the normal reading frame (see Fig. 1). For those transcripts that use the donor site of exon 5, the 101-base deletion creates an exon that is a fusion of exon 4, part of the intron between exon 4 and 5, and the remaining portion of exon 5. This fusion also creates a change in the translational reading frame which is +1 relative to normal (see Fig. 1). DNA sequence analysis (not shown) indicates that both classes of *Mhc*^{1} transcripts have a premature translation-termination codon within ~100 codons of the exon 4 border.

Since the sequence of the 5′ end of the MHC gene had been determined and the exon-intron structure characterized (Wassenberg et al., 1987; Kronert, W. A., and S. I. Bernstein, unpublished data), we were able to calculate the approximate molecular mass of the predicted truncated MHC proteins. The premature termination of translation that occurs in *Mhc*^{1} transcripts would produce MHC proteins of ~30 kD. It was important to determine whether these truncated MHC proteins are stable in order to understand the phenotype of the *Mhc*^{1} mutation. To examine this, thorax homogenates from *Mhc*^{1}/+ adults were electrophoresed on an SDS-polyacrylamide gel and compared to homogenates of wild-type thoraces. No protein bands accumulate in the mutant thoraces that fail to accumulate in wild-type (data not shown). To assay the short-term stability of truncated MHC proteins, we injected the thoraces of late stage *Mhc*^{1}/+ or *Canton-S* pupae with [^{35}S]methionine and allowed them to incubate for 1 h. We then homogenized the thoraces in SDS sample buffer and ran a portion on a polyacrylamide gel. After autoradiography of the fluorographed gel, no obvious truncated proteins were detected in the mutant compared to wild-type (data not shown). Thereore, *Mhc*^{1} truncated proteins do not accumulate to a detectable level.

Effect of the Mhc^{1} *Mutation on Muscle Structure*

Mhc^{1} homozygotes are capable of undergoing gastrulation but die at the late embryonic stage without displaying muscular movement (Mogami et al., 1986). The molecular characterization of *Mhc*^{1} suggests it is a null allele. We confirmed this by comparing the muscle structure of homozygous *Mhc*^{1} larvae (dissected from their eggs) to *Canton-S* larvae of the same developmental stage (Fig. 3). Transverse sections of *Canton-S* larvae show a relatively disorganized array of myofilaments typical of larval intersegmental muscle (Fig. 3 *a*). Thick and thin filaments are clearly visible within the developing muscle. Transverse sections of homozygous *Mhc*^{1} organisms (Fig. 3 *b*) indicate that the larval intersegmental muscles completely lack thick filaments while all other ultrastructural aspects of the cells appear normal. Examination of visceral muscle in homozygous *Mhc*^{1} larvae indicates it also completely lacks thick filaments (data not shown).

Longitudinal sections of homozygous *Canton-S* and *Mhc*^{1} larvae are shown in Fig. 3, *c* and *d*. In *Canton-S* larval intersegmental muscle, organized myofibrils containing well-organized Z-bands and interdigitating thick and thin fila-

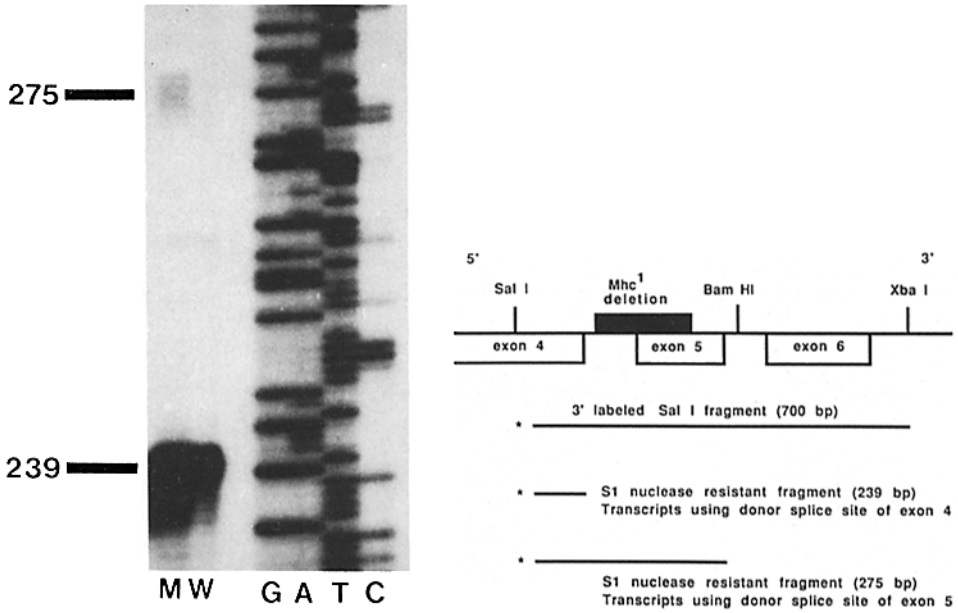

Figure 2. S1 nuclease analysis of transcripts from $Mhc^1/+$ heterozygotes reveals that the vast majority of transcripts use the donor splice site of exon 4 while a minority of Mhc^1 transcripts use the donor site of exon 5. The figure is an autoradiograph of a urea–polyacrylamide gel containing S1 nuclease–treated RNA–DNA hybrids. The DNA was labeled at an upstream Sal I site (Fig. 1), strand separated, and hybridized to pupal RNA. After hybridization and S1 nuclease treatment, two protected fragments were detected; one corresponding to 239 bases and the other to 275 bases. Both protected fragments were present after treatment of RNA isolated from $Mhc^1/+$ heterozygotes (lane *M*) but only the protected fragment of 239 bases was present after treatment of RNA isolated from wild-type (lane *W*). The band at 275 bases seen with the $Mhc^1/+$ RNA is very faint, indicating most Mhc^1 transcripts are using the donor site of exon 4. RNA was also isolated from homozygous Mhc^1 embryos and used in a S1 nuclease protection experiment. A similar ratio between the 239-base and 275-base fragments was seen (data not shown).

ments are apparent. Sarcomeres are in a contracted state and are 3 μm in length. In homozygous Mhc^1 larvae Z-bands are poorly organized. Sarcomeric structure is completely disrupted and no thick filaments are discernable. Other structural aspects of the cells appear normal. The ultrastructural phenotype of mutant embryos explains the embryonic lethality seen in homozygous Mhc^1 organisms.

Larval intersegmental muscle of $Mhc^1/+$ organisms functions adequately for locomotion as do muscles used in adult walking. These heterozygotes however, are unable to fly or jump. We were interested in the variable effect of the Mhc^1 mutation on muscle function since the known molecular lesion should affect all isoforms of MHC. We therefore used transmission EM to examine the ultrastructure of three different muscles in organisms with the $Mhc^1/+$ genotype. We selected the IFM, TDT, and larval intersegmental muscle since they represent some of the variety of muscle types seen in *Drosophila*. Larvae and adult thoraces of $Mhc^1/+$ heterozygotes were embedded in Spurr's resin, sectioned, stained, and then viewed under the transmission electron microscope. Comparisons were made between wild-type and mutant muscle structures. To assay changes in thick filament number in the well-delineated myofibrils of the IFM, we compared the number of thick filaments in wild-type and mutant myofibrils. We also analyzed reductions in thick filament number in each muscle type by counting the number of thin filaments surrounding a particular thick filament (an average value for 15 thick filaments was determined).

Fig. 4, *a* and *b*, show representative transverse sections of a single myofibril from the IFM of *Canton-S* and $Mhc^1/+$ heterozygotes. From the transverse section of *Canton-S* it can be seen that the myofibrils are cylindrical, having a diameter of ~1.5 μm. Interdigitating thick and thin filaments form a double hexagonal lattice with thin filaments occupying positions midway between each adjacent pair of thick filaments. Thick filaments of the IFM appear to possess a hollow core and are of uniform diameter. One striking feature of the lattice is its precise regularity, with each thick filament always surrounded by six thin filaments. Sarcoplasmic reticulum is sparse compared to other vertebrate and invertebrate muscle types. Large mitochondria fill the space between the individual myofibrils and glycogen granules are abundant. In a transverse section of a $Mhc^1/+$ heterozygote (Fig. 4 *b*), the precise double hexagonal array of interdigitating thick and thin filaments is disrupted. The filament arrangement in the center of the myofibril approaches that of the double hexagonal array seen in wild-type but peripheral regions of the myofibril become increasingly disorganized. Thick filament diameter is similar to that of wild-type, but there is ~50% reduction in the number of thick filaments per myofibril. This results in a decrease in the thick/thin filament ratio, with each thick filament being surrounded by an average of 9–10 thin filaments. Myofibril diameter in $Mhc^1/+$ heterozygotes is reduced by ~30% compared to wild-type.

Fig. 4, *c* and *d*, show longitudinal sections of myofibrils from the IFM of *Canton-S* and $Mhc^1/+$ heterozygotes. The longitudinal section of *Canton-S* IFM illustrates the interdigitating arrangement of thick and thin filaments. Sarcomere length is ~3 μm. The M-band is clearly demarcated by the presence of a well-defined band of glycogen granules. Wild-type myofibrils are discrete and remain this way throughout the length of the muscle fibers. Z-bands from adjacent myofibrils are not necessarily aligned in register. Fig. 4 *d* illustrates a longitudinal section of myofibrils from the IFM

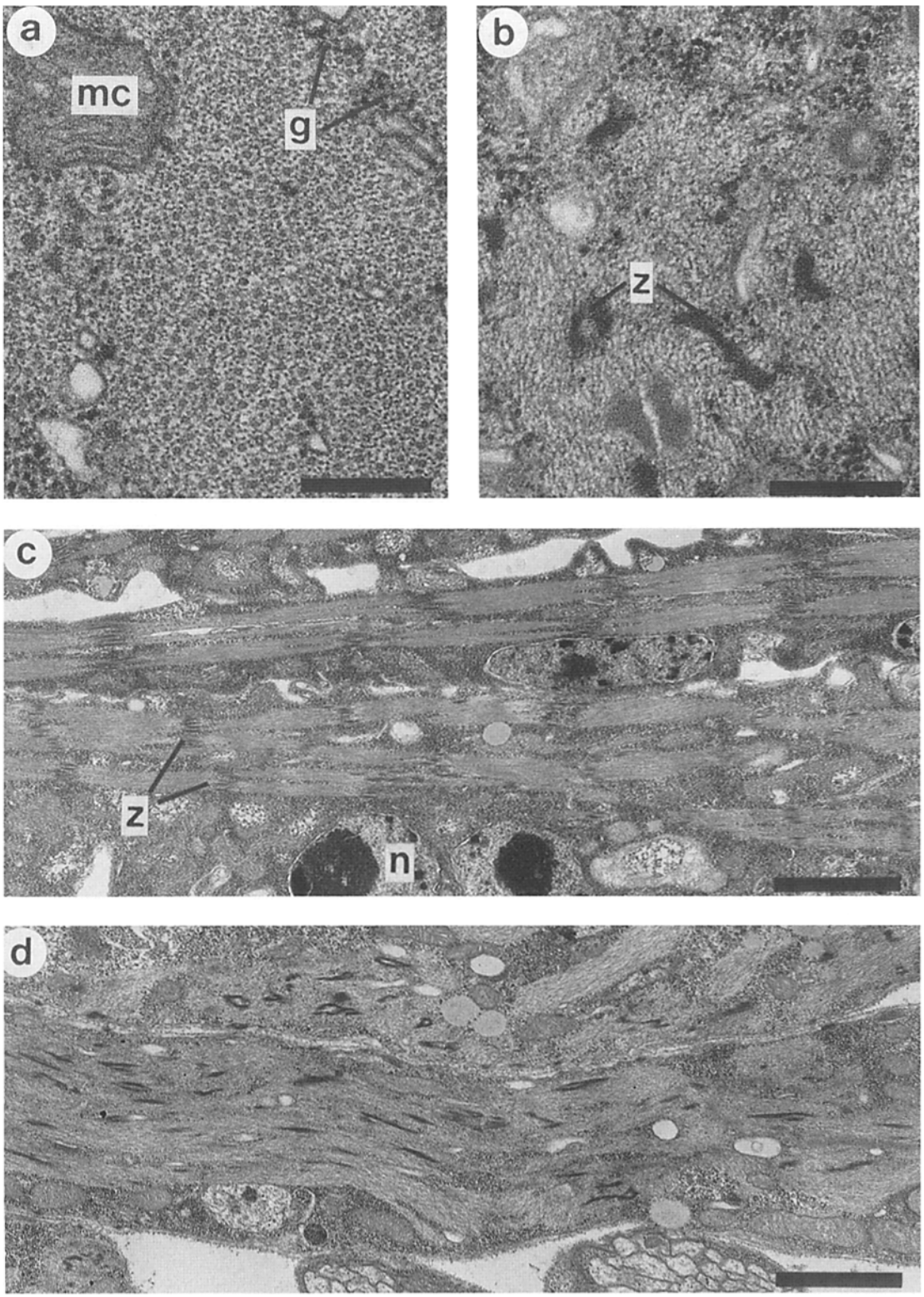

Figure 3. Ultrastructure of the embryonic intersegmental muscles. *a* and *b* are transverse sections through wild-type and homozygous *Mhc*^{1} myofibers. Small mitochondria (*mc*) and collections of glycogen granules (*g*) are present. In wild-type myofibers, thick and thin filaments are clearly present but are not well organized. In homozygous *Mhc*^{1} myofibers, thick filaments are completely absent. Areas containing Z-disc (*z*) material can be seen. *c* and *d* are longitudinal sections through wild-type and homozygous *Mhc*^{1} myofibers. Wild-type myofibers clearly possess a sarcomeric organization with visible Z-bands (*z*). Sarcomeres are contracted and are 3 μm in length. Many nuclei (*n*) can be found within the myofiber. Homozygous *Mhc*^{1} myofibers lack organized sarcomeres and Z-band material is poorly organized. Bars: (*a* and *b*) 0.25 μm; (*c* and *d*) 2 μm.

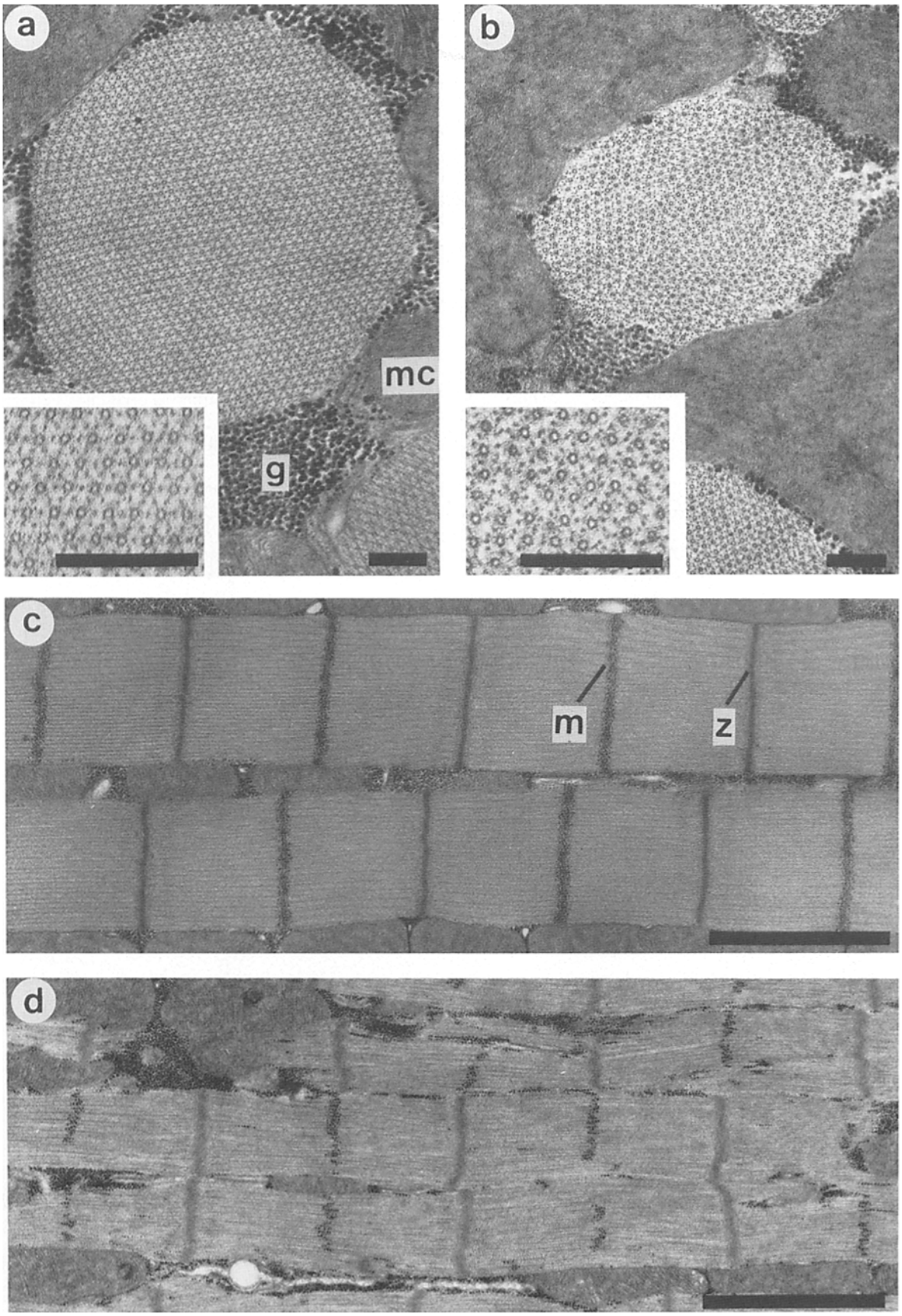

Figure 4. Ultrastructure of the IFM. *a* and *b* are transverse sections through wild-type and *Mhc*^{1}/+ myofibrils. Large mitochondria (*mc*) and collections of glycogen granules (*g*) surround the myofibrils. Myofilaments in the wild-type are organized in a rigid double hexagonal array. *Mhc*^{1}/+ myofibrils do not contain a regular array of myofilaments and each thick filament is surrounded by 9–10 thin filaments on average. *Mhc*^{1}/+ myofibril diameter is reduced ~30%. Thick filament diameter is similar to wild-type. *c* and *d* are longitudinal sections through wild-type and *Mhc*^{1}/+ myofibrils. Wild-type myofibrils remain discrete through the length of the myofiber and possess highly ordered sarcomeres with well-defined Z-bands (*z*) and M-bands (*m*). *Mhc*^{1}/+ myofibrils commonly branch, and gaps in the myofilament lattice are readily apparent. Z-bands and especially M-bands are poorly organized. Bars: (*a* and *b*) 0.2 μm; (*c* and *d*) 2 μm.

of *Mhc*^{1}/+ heterozygotes. Sarcomere length is similar to *Canton-S* myofibrils. Z-bands and especially M-bands are often poorly defined. Thick and thin filaments no longer appear to precisely interdigitate to give the highly ordered sarcomeres seen in *Canton-S* myofibrils, as gaps in the filament lattice are readily apparent. In addition, many myofibrils fail to remain discrete throughout the length of the muscle fiber; branching between adjacent myofibrils is common.

We also examined transverse sections of the TDT of wild-type and *Mhc*^{1}/+ heterozygotes (Fig. 5). The wild-type TDT muscle fibers contain large numbers of rectangular myofibrils which are delineated by an extensive system of sarcoplasmic reticulum (Fig. 5 *a*). Thick filaments, as in the IFM, possess hollow cores and are uniform in diameter although the filament lattice does not have the same precise regularity as the double hexagonal lattice of the IFM. However, thick filaments tend to be organized such that straight lines can be drawn through the center of a series of them. Each thick filament is surrounded by a variable number of thin filaments, usually 10–11. In *Mhc*^{1}/+ heterozygotes (Fig. 5 *b*) the thick/thin filament ratio is reduced as each thick filament is surrounded by an increased number of thin filaments (20 on average). Interestingly, the hollow core structure which is so apparent in the thick filaments of *Canton-S* appears to be missing in many of the thick filaments of *Mhc*^{1}/+ TDT muscle. In addition, thick filament diameter in the mutant TDT is not uniform and filaments are larger than those seen in the wild-type. Thick filaments are not arranged in the same array as in wild-type, as straight lines can no longer be drawn connecting their centers. The cross-sectional area of individual myofibrils of mutant TDT is generally reduced when compared to *Canton-S* myofibrils.

Figs. 6, *b* and *d*, show transverse sections of larval intersegmental muscle from *Canton-S* and *Mhc*^{1}/+ heterozygotes. W ild-type intersegmental muscle displays a lack of definition of individual myofibrils; instead the thick and thin filaments form large sheets. Sarcoplasmic reticulum is relatively sparse. Thick filaments, like those of the IFM and the TDT, are of a uniform size. The filament lattice is highly irregular with no obvious repeating pattern. Each thick filament is surrounded by a variable number of thin filaments usually 9–10. In *Mhc*^{1}/+ heterozygotes (Fig. 6 *d*) the thick/thin filament ratio is reduced resulting in each thick filament being surrounded on average by 20 thin filaments. In addition, the diameters of the thick filaments are variable, with many appearing much larger than wild-type.

Fig. 6, *a* and *c*, show representative longitudinal sections of third instar larval intersegmental muscle from *Canton-S* and *Mhc*^{1}/+ heterozygotes. The longitudinal section of the wild-type shows an area of fully stretched myofibrils and sar-

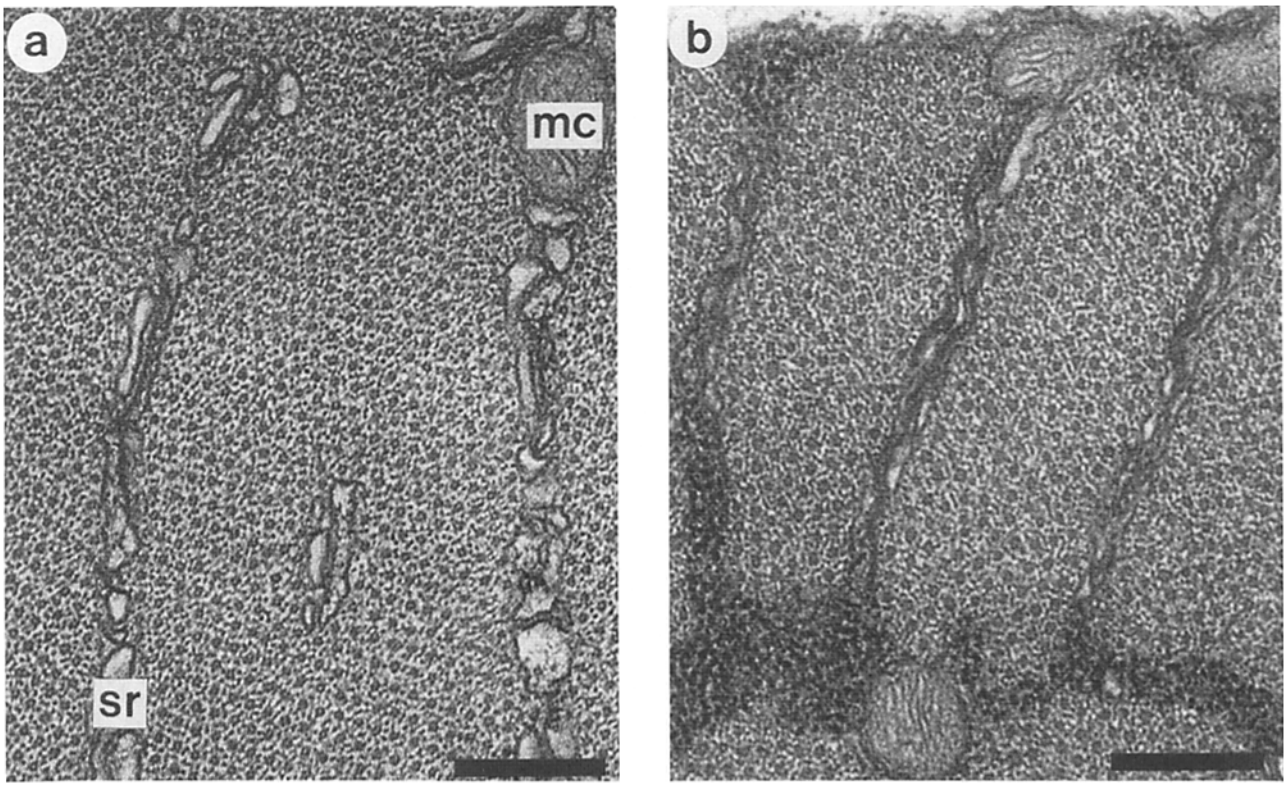

Figure 5. Ultrastructure of the TDT. Wild-type myofibers contain collections of myofibrils which are defined by an extensive system of sarcoplasmic reticulum (*sr*). Thick filaments form an ordered lattice in which lines can be drawn through the center of a series of them. Thick filaments are uniform in diameter and are surrounded by an average of 10–11 thick filaments. Small mitochondria are found between myofibrils and collections of glycogen granules are normally seen (the glycogen granules have been washed out of the wild-type myofiber shown in *a*). *Mhc*^{1}/+ myofibers contain myofibrils that are smaller in area and thick filaments are not arranged in an array such that straight lines can be drawn through a series of them. Mutant myofibrils contain thick filaments that are nonuniform in diameter. Each thick filament is surrounded by an average of 20 thin filaments. Bars, 0.25 μm.

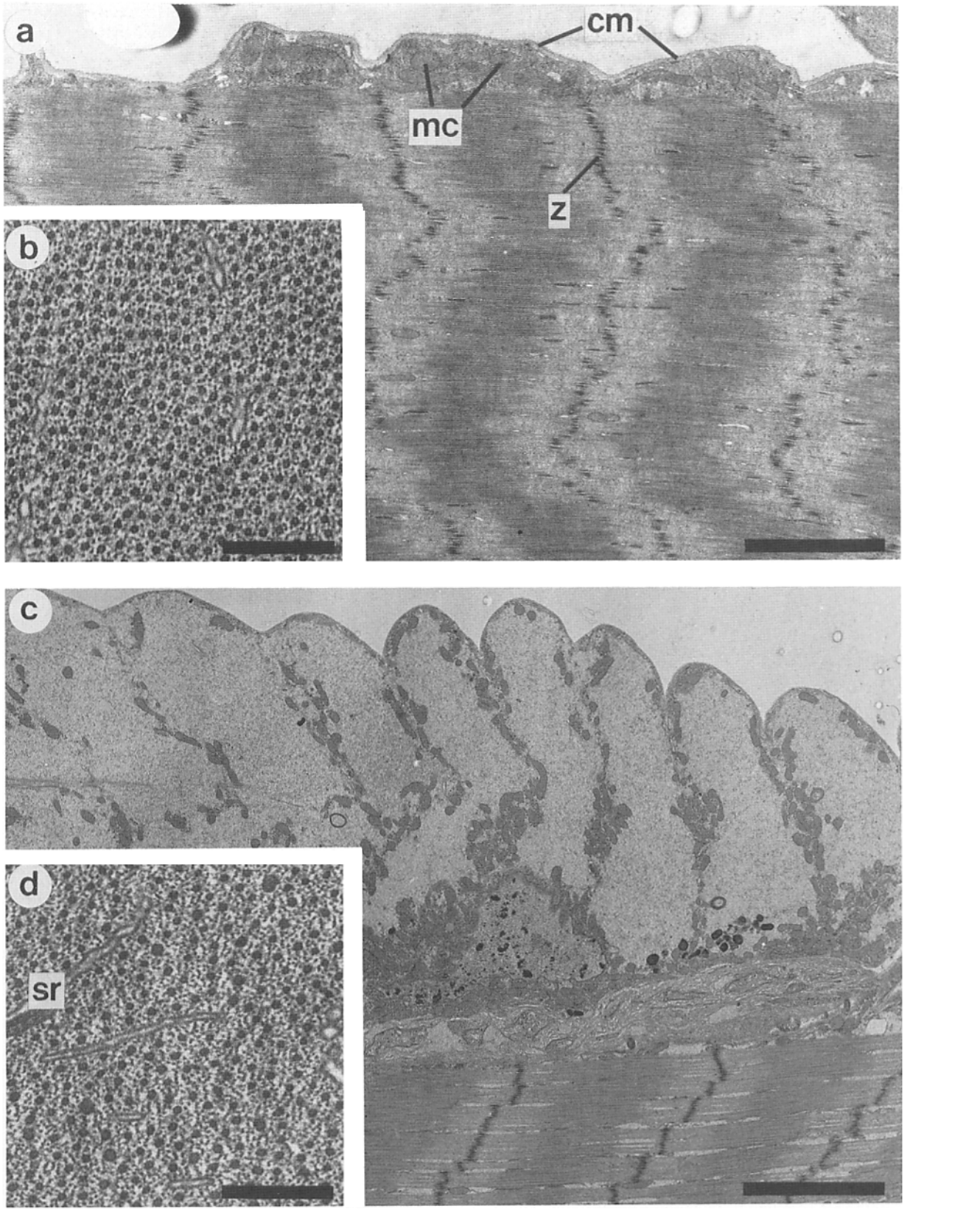

Figure 6. Ultrastructure of intersegmental muscles from third instar larvae. *b* and *d* are transverse sections of wild-type and $Mhc^1/+$ myofibers. Wild-type myofibers contain an array of poorly organized myofilaments. Thick filaments are of a uniform size and each thick filament is surrounded by an average of 9–10 thin filaments. Sarcoplasmic reticulum (*sr*) is sparse. $Mhc^1/+$ myofibers have a reduced number of thick filaments resulting in each thick filament being surrounded by an average of 20 thin filaments. Thick filaments in the mutant myofiber vary in diameter with some appearing much larger than wild-type. The distance between thick filaments in the mutant remains unchanged. *a* and *c* are longitudinal sections of wild-type and $Mhc^1/+$ myofibers. Wild-type myofibers contain sheets of poorly defined myofibrils which are aligned in register at the Z-band (*z*). The myofiber is fully stretched and sarcomere length is ~9 μm. The cell membrane (*cm*) is visible and collections of mitochondria (*mc*) can be found along its length. Mutant myofibers have a higher density of Z-bands. A large excess of cell membrane is loosely anchored at a series of points along its length. Collections of mitochondria and granular material are found in the area of excess membrane. Bars: (*a* and *c*) 5 μm; (*b* and *d*) 0.2 μm.

comere length is ~9 μm. Mitochondria within the myofilament lattice are thinly distributed but large collections are found at the periphery of the cell. Thin filaments are anchored in Z-bands and Z-bands appear in nearly complete registry. Longitudinal sections from *Mhc*^{1}/+ heterozygotes show an increased density of Z-band material. The volume of myofibrils within the cell is reduced resulting in an overabundance of cell membrane which is loosely anchored at a series of points along its length. Granular material is concentrated in areas lacking myofibrils causing the thin filaments of the myofibrils to appear more distinct. Sarcomere length appears unchanged and the myofibrils are in register.

The reduced volume of the contractile apparatus seen in *Mhc*^{1}/+ larvae results from an ~50% reduction in the number of thick filaments within the myofiber in conjunction with equivalent thick filament packing in mutant and wild-type muscles (Fig. 6, *b* and *d*). In light of the phenotype seen in longitudinal section of *Mhc*^{1}/+ heterozygotes, it is remarkable that the muscle functions adequately for larval movement.

Discussion

Biochemical and electron microscopic studies indicate invertebrate thick filaments consist of a core structure, about which a layer of paramyosin molecules, and in turn myosin molecules are organized (Epstein et al., 1985). Myosin itself is a large, hexameric protein composed of two heavy chain subunits (MHC), two alkali light chain subunits, and two regulatory light chain subunits (Weeds, 1969; Weeds and Lowey, 1971; Lowey and Risby, 1971). In *Drosophila*, the genes encoding the MHC (Bernstein et al., 1983; Rozek and Davidson, 1983), alkali light chain (Falkenthal et al., 1984), and regulatory light chain proteins (Parker et al., 1985) have been identified. A detailed molecular characterization of these genes and mutations affecting them offers a powerful approach to understanding thick filament assembly and function.

In this report, we have determined the molecular defect of the dominant-flightless mutation *Mhc*^{1} and illustrated its effect on IFM, TDT, and larval intersegmental muscle structure. The *Mhc*^{1} mutation is a 101-bp deletion in the MHC gene which results in the removal of most of exon 5 and the preceding intron. S1 nuclease mapping indicates that mutant transcripts follow two alternative processing pathways. Both pathways result in the production of mature transcripts with altered translation reading frames that should yield truncated MHC proteins with an approximate molecular mass of 30 kD. Analysis of thoracic proteins from *Mhc*^{1}/+ heterozygotes suggests the truncated MHC proteins are highly unstable. Homozygous *Mhc*^{1} embryos completely lack thick filaments in their developing muscles. Electron microscopic observation of heterozygous mutant muscle fibers demonstrates that the *Mhc*^{1} mutation reduces the number of thick filaments in all muscle types and alters thick filament shape and size in the TDT and larval intersegmental muscle. The observed ultrastructural abnormalities of *Mhc*^{1}/+ flies support our contention that *Mhc*^{1} is a null allele since its muscle ultrastructure is identical to that displayed by a deficiency heterozygote for the MHC gene region (data not shown).

The splicing pathway used by *Mhc*^{1} transcripts in vivo supports the conclusion of Reed and Maniatis (1986) that exon sequences play a critical role in determining splice site use. In their experiments, they demonstrated that large deletions or substitutions of human β-globin exon sequences usually inactivate the adjacent donor or acceptor splice site in precursors containing tandemly duplicated splice sites. They also showed that exclusive use of the closest donor or acceptor splice sites occurs in the absence of perturbations in exon sequences. The *Mhc*^{1} mutation deletes 40 of the 64 nucleotides of exon 5 creating a situation where the donor splice sites of exon 4 and 5 are competing for the acceptor splice site of exon 6. S1 nuclease mapping results indicate this change in exon 5 sequences nearly completely inactivates the donor site of exon 5 and the more distal donor site of exon 4 is used.

Our failure to detect the *Mhc*^{1} protein products in muscle cells indicates *Mhc*^{1} should behave as a null allele. This accounts for several previously described phenotypic characteristics of the *Mhc*^{1} mutation (Mogami et al., 1986). Lethality of homozygous *Mhc*^{1} embryos at the late embryonic stage apparently results from the failure to assemble any MHC into thick filaments. Resulting muscle dysfunction prevents larval emergence from the egg. The null effect of the *Mhc*^{1} mutation also explains why muscles of *Mhc*^{1}/+ heterozygotes possess 60% of wild-type amounts of MHC protein, levels similar to those of a haploid for the MHC gene. Lastly, the null phenotype of the *Mhc*^{1} mutation accounts for the ability of a MHC duplication (*Mhc*$^{+}$/*Mhc*$^{+}$/*Mhc*^{1}) to rescue the dominant-flightless phenotype. Products from the *Mhc*^{1} allele do not assemble into the myofibrillar apparatus and prevent function of the flight muscle fibers.

The null phenotype of the *Mhc*^{1} allele is understandable based on the nature of the mutation and known properties of the MHC protein. MHC is a multifunctional polypeptide with discrete domains. The carboxy-terminal half of MHC is rod-like and contributes to the backbone of the thick filament (McLachlan and Karn, 1982, 1983; McLachlan, 1983; Parry, 1981); the amino-terminal half of the molecule contributes to forming the globular head which possesses the ATPase and actin-binding activities (Szilagyi et al., 1979; Walker et al., 1982; Hozumi and Muhlad, 1981; Labbe et al., 1982; Sutoh, 1982). The rod portion of MHC is a repetitive alpha-helical sequence which creates a hydrophobic surface for the interactions between the two MHC subunits and in addition leads to electrostatic interactions between MHC dimers which are important in the assembly of these dimers into thick filaments (McLachlan and Karn, 1982, 1983). In light of the critical role MHC rod sequences play in myosin and thick filament assembly, our failure to detect truncated MHC protein in *Mhc*^{1}/+ heterozygotes was not unexpected. The *Mhc*^{1} mutation should lead to the production of MHC proteins that completely lack rod sequences. These rodless MHC proteins are likely to be highly unstable. Support for this hypothesis derives from studies of the stability of mutant MHC proteins in *C. elegans*. Dibb et al. (1985) have analyzed six mutations in the *unc*-54 MHC gene which cause premature termination of protein synthesis at different points within the rod region. While a mutant protein that is 61 residues shorter than wild-type accumulates to detectable levels in one mutant strain, truncated MHC proteins with more COOH-terminal residues removed are not detectable. Therefore, stability of sarcomeric myosins appears to require nearly complete rod sequences.

The ability to isolate homozygous *Mhc*^{1} larvae has provided the first opportunity to study the ultrastructural phenotype of muscle in the complete absence of MHC protein. Many null mutants for the *C. elegans* body wall MHC B gene have been described (Waterston et al., 1982) but none of these completely lack thick filaments (MacLeod et al., 1977*a*). This is due to the coexpression of a second MHC isoform encoded by the MHC A gene (Garcea et al., 1978). Our results show that no discernable thick filaments exist in muscles completely null for MHC. Assuming core and paramyosin proteins still accumulate in the *Mhc*^{1} homozygote, this result supports the concept that the diameter and shape of the thick filament in transverse section is largely due to the assembly of myosin molecules (Squire, 1981*a*). In addition, the abnormal ultrastructure of *Mhc*^{1} homozygotes suggests that sarcomere construction requires thick filaments which possess a normal complement of myosin molecules. In the absence of wild-type thick filaments, muscles contain disorganized interdigitating filaments with poorly organized Z-band material. The retarded sarcomere construction in MHC-null muscle raises the intriguing possibility that myosin–actin interaction plays a critical role in the assembly of the sarcomere. This idea is bolstered by the absence of sarcomeres in the IFM of a *Drosophila* actin mutant (Mahaffey et al., 1985).

The *Mhc*^{1} mutation exhibits a dominant effect on IFM and TDT function while other muscle types such as larval intersegmental muscle function adequately in heterozygotes (*Mhc*^{1}/+). Reduction in thick filament numbers is observed in all muscle types and directly correlates with the reduced levels of MHC protein that had been noted in earlier experiments (Mogami et al., 1986). Abnormally large thick filaments are common in the TDT and are especially apparent in the functional larval intersegmental muscle. These large thick filaments are similar to those described for some *C. elegans* mutants (Waterston et al., 1980) where it was shown that they result from an overaccumulation of paramyosin. Interestingly, thick filament diameter is similar to wild-type in the IFM of *Mhc*^{1}/+ organisms. This may be due to the relatively low levels of paramyosin found in IFM of insects with high wing-beat frequencies (Bullard et al., 1973). Our results show the differential sensitivity of various muscles to the *Mhc*^{1} allele is not a consequence of differential changes in thick filament number or structure.

The increased sensitivity of TDT and IFM function to alterations in contractile proteins can be accounted for by examining the structure of the myofilament array found in each of these muscles. In insect IFM, both the myosin molecules on the thick filament and their actin target sites on the thin filaments have been described as forming helices with a characteristic pitch (Reedy and Garrett, 1977; Squire, 1981*b*). These helices are arranged such that, when superimposed, a maximum number of potential myosin–actin interactions occur. This arrangement allows insect IFM to be highly efficient and capable of contracting at rates in excess of 300 Hz.

In IFM of *Mhc*^{1}/+ heterozygotes there is a nearly 50% reduction in MHC protein leading to a reduced number of thick filaments. The double hexagonal lattice is disrupted and an increased number of thin filaments surround each thick filament. The reduction in MHC content may alter the helical pattern of myosin molecules on the thick filament. In addition, the distance between thick and thin filaments is irregular. These changes prevent maximal interactions between myosin molecules and their actin target sites resulting in muscle dysfunction. A reduction in the number of potential myosin cross-bridges would also be expected to occur in the TDT, though its filament lattice is somewhat less structured.

The larval intersegmental muscle of *Mhc*^{1}/+ organisms also displays a reduced number of thick filaments. However, unlike the TDT and IFM, larval intersegmental muscle does not form a regular array of myofilaments with an obvious repeat pattern. The arrangement of the myofilaments is not designed to maximize myosin–actin interactions. Apparently, the interaction between myosin and its actin target sites in larval intersegmental muscle of *Mhc*^{1}/+ organisms is sufficient to allow this slow-contracting muscle to function.

Finally, we note that the *Mhc*^{1} allele has great potential for use in experiments designed to elucidate the function of different MHC isoforms, an important question not easily addressed in other systems. Sequencing of the MHC gene (Bernstein et al., 1983, 1986; Rozek and Davidson, 1983; Wassenberg et al., 1987), analysis of MHC mRNA expression (Bernstein et al., 1983, 1986; Rozek and Davidson, 1983, 1986), and examination of homozygous viable MHC mutations (our unpublished results) indicates that a complex pattern of alternative splicing of the wild-type MHC transcript exists. These splicing patterns can result in the tissue-specific accumulation of transcripts encoding different forms of MHC protein. *Mhc*^{1} organisms, because they are MHC null, are ideal recipients for germline transformation. P element–mediated germline transformation of MHC genes into *Mhc*^{1} recipients will permit us to determine if we can rescue the flightless phenotype of this mutant. Use of in vitro mutated MHC genes for germline transformation of *Mhc*^{1} organisms should allow us to examine the biological function of MHC domains encoded by alternatively spliced exons. For example, sequences which encode the different COOH termini of the MHC protein could be altered to conclusively demonstrate whether this domain plays a postulated critical role in controlling thick filament assembly (Bernstein et al., 1986; Rozek and Davidson, 1986).

We thank William Kronert for his excellent technical assistance in sequencing the *Mhc*^{1} gene. P. T. O'Donnell is indebted to K. Tokuyasu for providing training in electron microscopy and to Michael McCaffrey for his technical advice. We thank Herbert Lebherz, Norbert Hess, William Kronert, and K. David Becker for their critical suggestions concerning the manuscript.

This work was supported by research grants to S. I. Bernstein from the National Institutes of Health (GM-32443) and the Muscular Dystrophy Association. Funds were provided to P. T. O'Donnell from a Sigma Xi Grant-in-aid.

Received for publication 29 March 1988, and in revised form 26 July 1988.

References

Bernstein, S. I., C. J. Hansen, K. D. Becker, D. R. Wassenberg II, E. S. Roche, J. J. Donady, and C. P. Emerson, Jr. 1986. Alternative RNA splicing generates transcripts encoding a thorax-specific isoform of *Drosophila melanogaster* myosin heavy chain. *Mol. Cell. Biol.* 6:2511–2519.

Bernstein, S. I., K. Mogami, J. J. Donady, and C. P. Emerson, Jr. 1983. *Drosphila* muscle myosin heavy chain encoded by a single gene in a cluster of muscle mutations. *Nature (Lond.).* 302:393–397.

Bullard, B., B. Luke, and L. Winkelman. 1973. The paramyosin of insect flight muscle. *J. Mol. Biol.* 75:359–367.

Chapman, R. F. 1982. Locomotion. *In* The Insects, Structure and Function. Harvard University Press, Cambridge, MA. 169–196.

Crossley, A. C. 1968. The fine structure and mechanism of breakdown of larval intersegmental muscles in the blowfly *Calliphora erythrocephala*. *J. Insect Physiol.* 14:1389–1407.

Crossley, A. C. 1978. The morphology and development of the *Drosophila* muscular system. *In* The Genetics and Biology of *Drosophila*. Vol. 2b. M. Ashburner and T. R. F. Wright, editors. Academic Press Inc., Ltd., London. 499–560.

Cullen, M. J. 1974. The distribution of asynchronous muscle in insects with particular reference to the Hemiptera: an electron microscopy study. *J. Entomol. Ser. A Gen. Entomol.* 49:17–41.

Dibb, N. J., D. M. Brown, J. Karn, D. G. Moerman, S. L. Bolten, and R. H. Waterston. 1985. Sequence analysis of mutations that affect the synthesis, assembly, and enzymatic activity of the *unc*-54 myosin heavy chain of *Caenorhabditis elegans*. *J. Mol. Biol.* 183:543–551.

Epstein, H. F., D. M. Miller III, I. Ortiz, and G. C. Berliner. 1985. Myosin and paramyosin are organized about a newly identified core structure. *J. Cell Biol.* 100:904–915.

Falkenthal, S., V. P. Parker, W. W. Mattox, and N. Davidson. 1984. *Drosophila melanogaster* has only one myosin alkali light-chain gene which encodes a protein with considerable amino acid sequence homology to chicken myosin alkali light chains. *Mol. Cell. Biol.* 4:956–965.

Garamvolgyi, N. 1965*a*. The arrangement of the myofilaments in the insect flight muscle. I. *J. Ultrastruct. Res.* 13:409–424.

Garamvolgyi, N. 1965*b*. The arrangement of the myofilaments in the insect flight muscle. II. *J. Ultrastruct. Res.* 13:425–434.

Garcea, R. C., F. Schachat, and H. F. Epstein. 1978. Coordinate synthesis of two myosins in wild-type and mutant nematode muscle during larval development. *Cell.* 15:421–428.

Hozumi, T., and A. Muhlad. 1981. Reactive lysyl of myosin subfragment 1: location of the 27K fragment and labeling properties. *Biochemistry.* 20: 2945–2950.

Karlik, C. C., and E. A. Fyrberg. 1985. An insertion within a variably spliced *Drosophila* tropomyosin gene blocks accumulation of only one encoded isoform. *Cell.* 41:57–66.

Karlik, C. C., M. D. Coutu, and E. A. Fyrberg. 1984. A nonsense mutation within the Act 88F actin gene disrupts myofibril formation in *Drosophila* indirect flight muscles. *Cell.* 38:711–719.

Labbe, J. P., D. Mornet, G. Roseau, and R. Kassab. 1982. Cross-linking of F-actin to skeletal muscle myosin subfragment 1 with bis (imido esters): further evidence for the interaction of myosin-head heavy chain with an actin dimer. *Biochemistry.* 21:6897–6902.

Laemmli, U. K. 1970. Cleavage of structural proteins during the assembly of the head of bacteriophage T4. *Nature (Lond.).* 227:680–685.

Landel, C. P., M. Krause, R. H. Waterston, and D. Hirsh. 1984. DNA rearrangements of the actin gene cluster in *Caenorhabditis elegans* accompany reversion of three muscle mutants. *J. Mol. Biol.* 180:497–513.

Lowey, S., and D. Risby. 1971. Light chains from fast and slow muscle myosins. *Nature (Lond.).* 234:81–84.

Mackenzie, J. M., Jr., R. L. Garcea, J. M. Zengel, and H. F. Epstein. 1978. Muscle development in *Caenorhabditis elegans*: mutants exhibiting retarded sarcomere construction. *Cell.* 15:751–762.

MacLeod, A. R., R. H. Waterston, R. M. Fishpool, and S. Brenner. 1977*a*. Identification of the structural gene for a myosin heavy-chain in *Caenorhabditis elegans*. *J. Mol. Biol.* 114:133–140.

MacLeod, A. R., R. H. Waterston, and S. Brenner. 1977*b*. An internal deletion mutant of a myosin heavy chain in *Caenorhabditis elegans*. *Proc. Natl. Acad. Sci. USA.* 74:5336–5340.

Mahaffey, J. W., M. D. Coutu, E. A. Fyrberg, and W. Inwood. 1985. The flightless mutant *raised* has two distinct genetic lesions affecting accumulation of myofibrillar proteins in flight muscles. *Cell.* 40:101–110.

Maniatis, T., E. F. Fritsch, and J. Sambrook. 1982. Molecular Cloning: A Laboratory Manual. Cold Spring Harbor Laboratory, Cold Spring Harbor, NY. pp. 545.

Maxam, A. M., and W. Gilbert. 1980. Sequencing end-labelled DNA with base-specific chemical cleavages. *Methods Enzymol.* 65:499–560.

McLachlan, A. D. 1983. Analysis of gene duplication repeats in the myosin rod. *J. Mol.Biol.* 169:15–30.

McLachlan, A. D., and J. Karn. 1982. Periodic charge distributions in the myosin rod amino acid sequence match cross-bridge spacings in muscle. *Nature (Lond.).* 299:226–231.

McLachlan, A. D., and J. Karn. 1983. Periodic features in the amino acid sequence of nematode myosin rod. *J. Mol. Biol.* 164:605–626.

Miller, A. 1950. The internal anatomy and histology of the imago of *Drosophila melanogaster*. *In* The Biology of Drosophila. M. Demerec, editor. John Wiley & Sons, New York. 468–480.

Mogami, K., and Y. Hotta. 1981. Isolation of *Drosophila* flightless mutants which affect myofibrillar proteins of indirect flight muscle. *Mol. & Gen. Genet.* 183:409–417.

Mogami, K., Y. Nonomura, and Y. Hotta. 1981. Electron microscopic and electrophoretic studies of a *Drosophila* muscle mutant *wings-up* B. *Jpn. J. Genet.* 56:51–65.

Mogami, K., P. T. O'Donnell, S. I. Bernstein, T. R. F. Wright, and C. P. Emerson, Jr. 1986. Mutations of the *Drosophila* myosin heavy-chain gene: effects on transcription, myosin accumulation, and muscle function. *Proc. Natl. Acad. Sci. USA.* 83:1393–1397.

Nachtigall, W., and D. M. Wilson. 1967. Neuromuscular control of Dipteran flight. *J. Exp. Biol.* 47:77–97.

Parker, V. P., S. Falkenthal, and N. Davidson. 1985. Characterization of the myosin light-chain-2 gene of *Drosophila melanogaster*. *Mol. Cell. Biol.* 5:3058–3068.

Parry, D. A. D. 1981. Structure of rabbit skeletal myosin. Analysis of amino acid sequences of two fragments from the rod region. *J. Mol. Biol.* 153: 459–464.

Peristianis, G. C., and D. W. Gregory. 1970. Early stages of flight muscle development in the blowfly *Lucilia cuprina*: a light and electron microscopy study. *J. Insect Physiol.* 17:1005-1022.

Pringle, J. W. S. 1967. The contractile mechanism of insect fibrillar muscle. *Prog. Biophys. Mol. Biol.* 17:1–60.

Reed, R., and T. Maniatis. 1986. A role for exon sequences and splice-site proximity in splice-site selection. *Cell.* 46:681–690.

Reedy, M. K., and W. E. Garrett. 1977. Electron microscopic studies of *Lethocerus* flight muscle in rigor. *In* Insect Flight Muscle. R.T. Tregear, editor. North-Holland Publishing Co., New York. 115–136.

Rozek, C. E., and N. Davidson. 1983. *Drosophila* has one myosin heavy chain gene with three developmentally regulated transcripts. *Cell.* 32:23–34.

Rozek, C. E., and N. Davidson. 1986. Differential processing of RNA transcribed from the single-copy *Drosophila* myosin heavy chain gene produces four mRNA's that encode two polypeptides. *Proc. Natl. Acad. Sci. USA.* 83:2128–2132.

Shafiq, S. A. 1963*a*. Electron microscopic studies on the indirect flight muscles of *Drosophila melanogaster*. I. Structure of the myofibrils. *J. Cell Biol.* 17:351–362.

Shafiq, S. A. 1963*b*. Electron microscopic studies on the indirect flight muscles of *Drosophila melanogaster*. II. Differentiation of the myofibrils. *J. Cell Biol.* 17:363–373.

Smith, D. S. 1963.The structure of flight muscle sarcosomes in the blowfly *Calliphora erythrocephala*. *J. Cell Biol.* 19:115–138.

Spurr, A. R. 1969. A low-viscosity epoxy resin embedding medium for electron microscopy. *J. Ultrastruct. Res.* 26:31–43.

Squire, J. 1981*a*. Molecular packing in myosin-containing filaments. *In* The Structural Basis of Muscle Contraction. Plenum Press, New York. 471–522.

Squire, J. 1981*b*. Comparative ultrastructures of diverse muscle types. *In* The Structural Basis of Muscle Contraction. Plenum Press, New York. 381–469.

Sutoh, K. 1982. Identification of myosin-binding on the actin-sequence. *Biochemistry.* 21:3654–3661.

Szilagyi, L., M. Balint, F. A. Sreter, and J. Gergely. 1979. Photoaffinity labeling with an ATP analog of the *N*-terminal peptide of myosin. *Biochem. Biophys. Res. Commun.* 87:936–945.

Thorson, J., and D. C. S. White. 1969. Distributed representations for actin–myosin interaction in the oscillatory contraction of muscle. *Biophys. J.* 9:360–390.

Toselli, P. A., and F. A. Pepe. 1968*a*. The fine structure of the ventral intersegmental abdominal muscles of the insect, *Rhodnius prolixus*, during the molting cycle. I. Muscle structure at molting. *J. Cell Biol.* 37:445–461.

Toselli, P. A., and F. A. Pepe. 1968*b*. The fine structure of the ventral intersegmental abdominal muscles of the insect, *Rhodnius prolixus*, during the molting cycle. II. Muscle changes in preparation for molting. *J. Cell Biol.* 37:462–481.

Tregear, R. T. 1975.The biophysics of fibrillar flight muscle. *In* Insect Muscle. P. N. R. Usherwood, editor. Academic Press, New York. 357–403.

Walker, J. E., M. Saraste, M. J. Runswick, and N. J. Gay. 1982. Distantly related sequences in the alpha and beta-subunits of ATP synthase, myosin, kinases and other ATP-requiring enzymes and a common nucleotide binding fold. *EMBO (Eur. Mol. Biol. Organ.) J.* 1:945–951.

Wassenberg II, D. R., W. A. Kronert, P. T. O'Donnell, and S. I. Bernstein. 1987. Analysis of the 5′ end of the *Drosophila* muscle myosin heavy chain gene: alternatively spliced transcripts initiate at a single site and intron locations are conserved compared to myosin genes of other organisms. *J. Biol. Chem.* 262:10741–10747.

Waterston, R. H., R. M. Fishpool, and S. Brenner. 1977. Mutants affecting paramyosin in *Caenorhabditis elegans*. *J. Mol. Biol.* 117:679–697.

Waterston, R. H., D. Hirsh, and T. R. Lane. 1984. Dominant mutations affecting muscle structure in *Caenorhabditis elegans* map near the actin gene cluster. *J. Mol. Biol.* 180:473–496.

Waterston, R. H., K. C. Smith, and D. G. Moerman. 1982. Genetic fine structure analysis of the myosin heavy chain gene *unc*-54 of *Caenorhabditis elegans*. *J. Mol. Biol.* 158:1–15.

Waterston, R. H., J. N. Thomson, and S. Brenner. 1980. Mutants with altered muscle structure in *Caenorhabditis elegans*. *Dev. Biol.* 77:271–302.

Weeds, A. G. 1969. Light chains of myosin. *Nature (Lond.).* 223:1362–1364.

Weeds, A. G., and S. Lowey. 1971. Substructure of the myosin molecule. II. The light chains of myosin. *J. Mol. Biol.* 61:701–725.